Sulfur impurities in CO_x feed gases of solid oxide cells: Effect on degradation and removal strategies

Matthias Riegraf[a], Katherine Develos-Bagarinao[b], Indro Biswas[a], and Rémi Costa[a]

[a]German Aerospace Centre (DLR), Institute of Engineering Thermodynamics, Pfaffenwaldring 38-40, 70569 Stuttgart, Germany
[b]Global Zero Emission Research Center, National Institute of Advanced Industrial Science and Technology, Tsukuba, Ibaraki 305-8569, Japan

Abstract

High-temperature solid oxide cells (SOC) offer unrivaled Faradaic and energetic efficiencies for carbon dioxide electrolysis. However, it is yet unclear which contaminant level in carbon monoxide and carbon dioxide feed gases are tolerable to achieve low degradation rates. In this work, electrolyte-supported cells (ESC) with Ni/Gadolinia-doped ceria (Ni/CGO) fuel electrodes were exposed to CO/CO_2 gas mixtures at open circuit voltage. The resistance evolution over time was monitored by means of electrochemical impedance spectroscopy. With this approach it is shown that a degradation over times of up to 96 h occurs. X-ray photoemission spectroscopy (XPS) and high-resolution secondary ion mass spectrometry (SIMS) imaging techniques were used to show that the degradation is related to sulfur impurities on the electrode surface. The results demonstrate the importance of feed gas purity for the commercialization of high-temperature CO_2 electrolysis.

Introduction

Solid oxide electrolysis cells (SOEC) are operated at high temperatures between 600 and 900 °C, which has the advantage of favorable kinetics and thermodynamics. In addition, they enable the operation in steam electrolysis, co-electrolysis and carbon dioxide electrolysis. Considerable progress has been made with regards to their durability in recent years to the extent that the major degradation phenomena are now often related to external impurities rather than to microstructural degradation of the electrodes. In particular, the poisoning of the nickel surface in the state-of-the-art Ni/cermet fuel electrodes is often observed. For example, sulfur impurities in CO_2 sources were reported to cause performance drops and increases in degradation rates in CO_2 electrolysis (1-5). However, so far these reports exclusively stem from the Technical University of Denmark (DTU), whereas not a single of the other large number of publications about high-temperature CO_2 electrolysis has reported such an issue. Furthermore, in all reports fuel-electrode-supported cells with a Ni/yttria-stabilized zirconia (YSZ) fuel electrode were used. This type of electrode is well-known to be particularly vulnerable towards poisoning in solid oxide fuel cell (SOFC) operation. By contrast, Ni/Gadolinia-doped ceria

(CGO) fuel electrodes were reported to display a higher tolerance towards sulfur poisoning (6-9). However, their application in CO_2 electrolysis has not been examined in detail so far.

Thus, in the present work an investigation of the stability of electrolyte-supported cells (ESC) with Ni/CGO fuel electrodes in CO/CO_2 gas mixtures is carried out.

Experimental Procedure

State-of-the-art electrolyte-supported cells with a size of 5x5 cm^2 and an active area of 4x4 cm^2 were supplied by Sunfire GmbH (Dresden, Germany). They consisted of a 90 µm thick 3 mol% Y_2O_3-doped ZrO_2 (3YSZ) electrolyte, 5 µm thick CGO interlayers on both the fuel and oxygen electrode side, a Ni/CGO fuel electrode with a functional layer and a current collector layer with increased Ni content, and an $La_{0.6}Sr_{0.4}Co_{0.2}Fe_{0.8}O_{3-\delta}$ (LSCF)/CGO oxygen electrode with LSCF current collector layer.

The setup for cell testing with up to four positions in the same test rig has been described in detail in previous studies (6, 10). All cells were operated at 860 °C at constant total fuel and air flow rates of 1 standard liter per minute (SLPM), respectively. Proper sealing of all cells was ensured by confirming the open circuit voltage (OCV) to be higher than 1.2 V in pure hydrogen and air.

During electrochemical testing, the change of the polarization resistance over time was investigated for different gas mixtures at open circuit voltage (OCV). Impedance spectra were recorded directly after switching to the nominal gas mixture and after operation in the respective mixture at different times (0 h, 1 h, 2 h, 4 h, 8 h, 12 h, 24 h, 48 h, 72 h, 84 h, 96 h). Carbon monoxide with a purity of 99.0 % and CO_2 with a purity of 99.995 % was used in all experiments both supplied by Linde AG (München, Germany).

For post mortem analysis, a cell was operated at 860 °C in 80 % CO_2, 20 % CO at OCV for ~140 h, then cooled down to 500 °C and eventually cooled down to room temperature in 2.5 % H_2, 97.5 % N_2. A reference sample was just reduced at 860 °C for 2 h in pure hydrogen, and subsequently cooled down to room temperature in 5 % H_2.

The surface chemistry was investigated with X-ray photoemission spectroscopy (XPS) in a vacuum system with a base pressure of $2x10^{-10}$ mbar, using a monochromated Al Ka source with an X-ray energy of 1486.74 eV and a hemispherical analyser (ESCALAB Xi+, FEI / ThermoFisher Scientific). The peak shape analysis was performed with Unifit 2016, applying convoluted Gaussian/Lorentzian profiles and a Shirley background function (11-13). The surface stoichiometry of the occurring atoms/signals was determined by the numerically fitted peak areas, photoionization cross sections by Yeh and Lindau (14), and instrumental transmission functions by the manufacturer. The energy axis of the system was calibrated by adjusting the reference signal of an ion-etched clean silver surface.

The elemental distribution across the cross-sectional surfaces of the reduced and tested samples was assessed by means of a high-resolution secondary ion mass spectrometry imaging analysis apparatus (SIMS, NanoSIMS 50L, Ametek CAMECA). The samples were first infiltrated with a high-vacuum-compatible resin and afterwards embedded into the NanoSIMS-specific sample holder using an alloy of Bi-Sn. The exposed surfaces were subsequently polished using diamond slurry and lightly coated with osmium to improve conductivity. The primary ion was Cs^+ with a minimum beam diameter of 50 nm and beam current of ~23 nA. For the measurements, raster areas were set at 20 µm x 20 µm and 10 µm x 10 µm. Secondary ion mass species of $^{16}O^-$, $^{32}S^-$, $^{58}Ni^-$, and $^{140}Ce^{16}O^-$ were analyzed simultaneously with a multicollection system. Image processing was carried out with the WinImage ver. 4.6 software (Ametek, Cameca).

Results and Discussion

Exposure of the Ni/CGO fuel electrode to a 80% CO_2, 20% CO feed gas mixture at OCV and 860°C over 96 h led to a significant increase of the polarization resistance at frequencies of ~1 Hz (Fig. 1), which was reported to be associated with a Ni/CGO surface process (6, 15). The degradation leveled off after approximately 48 h as shown in the plot of the polarization resistance over time in Figure 2. Since the experiment was carried out at OCV, the degradation was likely correlated with a purely catalytic phenomenon. In our previous work, cells of the same type were shown to be thermo-chemically stable in hydrogen-fueled fuel cell durability tests with the absence of Ni/CGO fuel electrode degradation (16, 17). Hence, the degradation was probably due to impurities in the feed gas.

The small increase of the ohmic resistance in Fig. 1 was most likely caused by the change from pure hydrogen to a CO/CO_2 gas mixture before the first impedance measurement, which led to a different pO_2 partial pressure in the fuel electrode compartment. Such an increase was reported to entail an increase in ohmic resistance due to its detrimental effect on the electrical conductivity of the CGO interlayer between electrolyte and fuel electrode (10).

The observed behavior of the polarization resistance in Figure 2 is very similar to CO_2 electrolysis experiments on Ni/YSZ-based cells where the increase of the Ni/YSZ charge transfer resistance was correlated with Ni surface poisoning by sulfur impurities from the CO_2 feed gas (2, 3).

In a previous work, we poisoned Ni/CGO-based solid oxide fuel cells with sulfur in a similar cell architecture in a similar test rig with the same cell housing (10). In such an environment, the performance during sulfur poisoning with 1 ppm hydrogen sulfide displayed the same saturation behavior as the cell in the present study. However, the poisoning progression leveled off after approximately 5 h. The performance decrease in the present study required about 50 h to finish. The sulfur impurity concentration can be calculated according to

$$p_S = \frac{\Gamma_{Ni}\, A}{\dot{V}\, t} \qquad [1]$$

with Γ_{Ni} being the active Ni surface site density (in mol·m^{-2}), A the surface area (in m^2), $\dot{V}$ the fuel gas flow rate (in m^3·s^{-1}) and t the saturation time (in s). Under the assumption of an equal Ni surface area of the two cells and adsorption of all sulfur atoms on the Ni surface, a total sulfur impurity level in the order of magnitude of ~100 ppb can be estimated for the present study. According to legal requirements, total sulfur concentration in food grade CO_2 cannot exceed 100 ppb (18). Nonetheless, they are most likely still present at lower concentrations. Carbonyl sulfide (COS) and carbon disulfide (CS_2) have been observed in concentrations of up to 20 ppb in CO_2 with food-grade quality (1, 18). These values are in the same order of magnitude as the value estimated above.

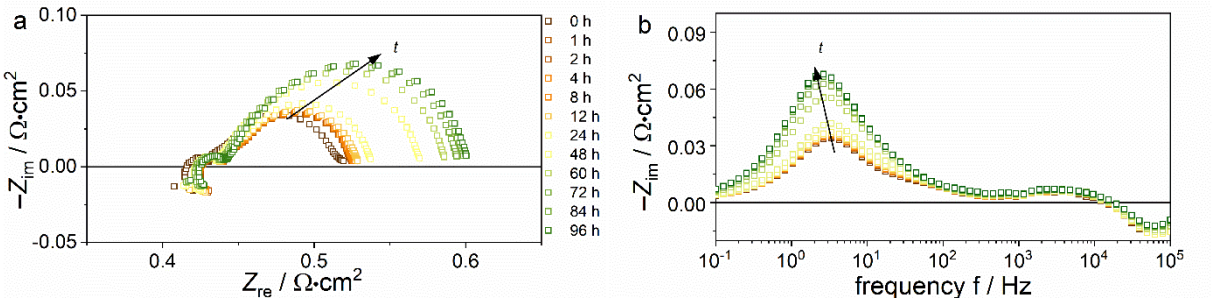

Figure 1. (a) Nyquist and (b) imaginary impedance plot of spectra recorded at 860 °C and OCV at different time points after switching to an 80% CO_2, 20% CO gas atmosphere. Adapted with permission from Ref.(19). Copyright 2023, Elsevier.

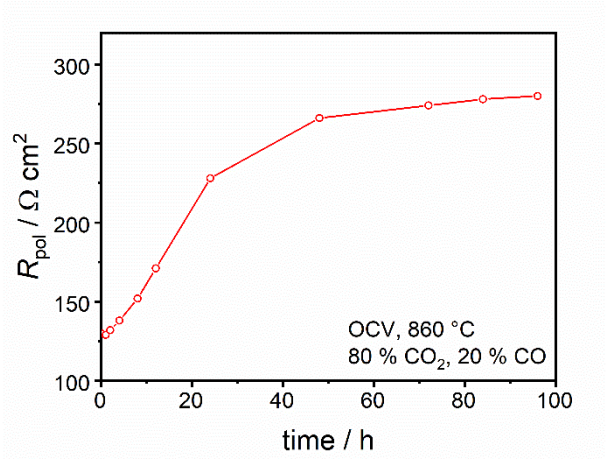

Figure 2. Evolution of the polarization resistance of the full cell over 96 h.

From studies of sulfur poisoning in SOFC it is known that sulfur is generally chemisorbed on the Ni surface at typical operating temperatures. Nickel sulfide species were shown to not form at H_2S concentrations below 100 ppm and temperatures above 600 °C (20, 21). Nevertheless, different nickel sulfides (Ni_3S_2, NiS, Ni_3S_4) have been observed to form in Ni/cermet electrodes at lower temperatures, consistent with the thermodynamically expected behavior (20, 22). In the present study, exposing the electrode to CO/CO_2 at 860°C and subsequent cooling in forming gas would probably lead to the desorption of sulfur impurities

from the electrode surface during the cooling process. Moreover, cooling down in CO/CO_2 atmosphere would have the risk of carbon formation via the Boudouard reaction at lower temperatures. Therefore, a sample was exposed to 80% CO_2, 20% CO at OCV and 860 °C for 144 h and cooled down until 500 °C in the same atmosphere where carbon formation is still thermodynamically unfavorable. Subsequently, the sample was cooled down to room temperature in 2.5% H_2, 97.5% N_2. Although the last cooling step posed the risk of sulfur desorption from the electrode surface, the kinetics of this desorption process at lower temperature was most likely drastically reduced.

After cooling down, the fuel electrode of the CO/CO_2-exposed sample was investigated by XPS and compared to a reference sample that was only reduced at 860 °C. The surface chemistry of these two Ni/CGO electrodes showed the signals of nickel, cerium, gadolinium and oxygen. The spectral region between 135 eV and 175 eV with the most prominent sulfur signals (electrons from S2p orbitals) is shown in Figure 3. Silica traces (Si 2s, 152.7 eV) were detected, which could stem from impurities in the raw materials. Sulfate and sulfide signals were detected on both sample surfaces, however, with a significantly higher concentration on the CO/CO_2 operated sample suggesting the presence of sulfur contaminants in the feed gas.

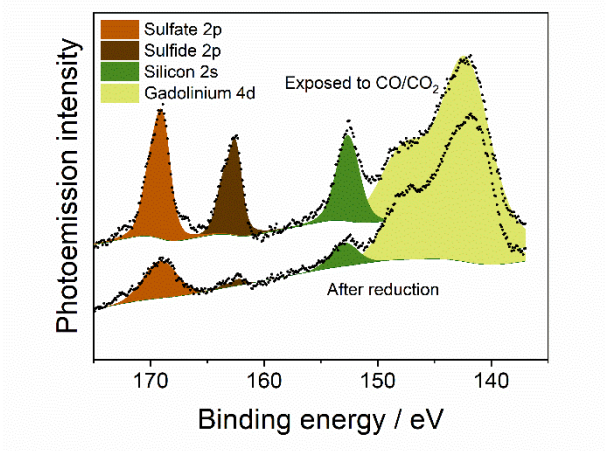

Figure 3. Photoemission spectra of the sulfate 2p and sulfide 2p region with a binding energy of 135-175 eV. Adapted with permission from Ref.(19). Copyright 2023, Elsevier.

Moreover, the samples were also investigated using high-resolution SIMS imaging, which allows the visualization of the distribution of trace contaminants on surfaces. Figure 4 shows the elemental mapping with the distribution of sulfur ($^{32}S^-$) in the reduced and the CO_2-exposed samples. To enable a semi-quantitative comparison, the secondary ion intensities of $^{32}S^-$ were normalized by $^{16}O^-$, that is, the mapping results were based on $^{32}S^-/^{16}O^-$ values in each sample. The results confirm a higher amount of sulfur deposited for the CO_2/CO-exposed sample compared to the reduced sample, showing good agreement with the XPS results.

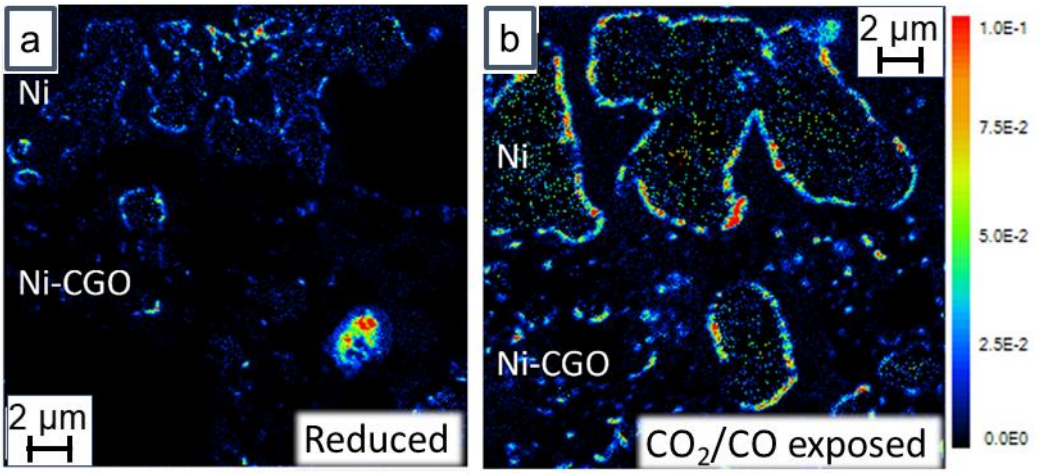

Figure 4. SIMS elemental mapping with the distribution of normalized intensities of sulfur ($^{32}S^-/^{16}O^-$) of the Ni/CGO electrode for the (a) reduced and (b) the CO/CO_2-exposed samples. a, b: 20 µm raster size. Adapted with permission from Ref.(19). Copyright 2023, Elsevier.

Summary and Conclusions

The present study demonstrates that sulfur impurities in the ppb level in CO_x gases can cause performance drops in CO_2 electrolysis. The degradation is related to an increase of the Ni/CGO electrode surface process impedance and led to polarization resistance increases of up to 150 mΩ cm^2. Analysis by XPS and a high-resolution SIMS imaging technique has unequivocally demonstrated that the mechanism is sulfur-induced electrode surface poisoning.

Acknowledgements

The German Ministry of Education and Research (BMBF) is acknowledged for funding in the framework of the “Kopernikus P2X-II” project under grant number 03SFK2E0-2. Chen-Yu Tsai and Christian Geipel from Sunfire GmbH are acknowledged for the supply of cells and helpful discussions. The authors are grateful to Kim Mehnert for contributions in sample preparation and evaluation for photoemission spectroscopic investigations.

References

1. A. Hauch, M. L. Traulsen, R. Küngas, and T. L. Skafte, *J. Power Sources,* **506,** 230108 (2021).
2. S. D. Ebbesen and M. Mogensen, *Electrochem. Solid-State Lett.*, **13**, B106 (2010).
3. S. D. Ebbesen and M. Mogensen, *J. Power Sources*, **193**, 349 (2009).
4. T. L. Skafte, P. Blennow, J. Hjelm, and C. Graves, *J. Power Sources,* **373,** 54 (2018).
5. S. D. Ebbesen, C. Graves, A. Hauch, S. H. Jensen, and M. Mogensen, *J. Electrochem. Soc.*, **157**, B1419 (2010).
6. M. Riegraf, M. P. Hoerlein, R. Costa, G. Schiller, and K. A. Friedrich, *ACS Catalysis*, **7**, 7760 (2017).
7. S. Kavurucu Schubert, M. Kusnezoff, A. Michaelis, and S. I. Bredikhin, *J. Power Sources*, **217,** 364 (2012).
8. W. C. Chueh, Y. Hao, W. Jung, and S. M. Haile, *Nature Materials*, **11**, 155 (2012).

9. M. Riegraf, A. Zekri, M. Knipper, R. Costa, G. Schiller, and K. A. Friedrich, *J. Power Sources,* **380,** 26 (2018).
10. M. Riegraf, V. Yurkiv, R. Costa, G. Schiller, and K. A. Friedrich, *ChemSusChem,* **10**, 587 (2017).
11. R. Hesse, T. Chassé, and R. Szargan, *Fresenius' journal of analytical chemistry,* **365**, 48 (1999).
12. D. A. Shirley, *Physical Review B,* **5**, 4709 (1972).
13. A. Proctor and P. M. Sherwood, *Anal. Chem.,* **54**, 13 (1982).
14. J. Yeh and I. Lindau, *At. Data Nucl. Data Tables,* **32**, 1 (1985).
15. M. Riedel, M. P. Heddrich, A. Ansar, Q. Fang, L. Blum, and K. A. Friedrich, *J. Power Sources*, **475,** 228682 (2020).
16. M. Riegraf, I. Bombarda, F. Dömling, T. Liensdorf, C. Sitzmann, N. Langhof, S. Schafföner, F. Han, N. Sata, C. Geipel, C. Walter, and R. Costa, *ACS Applied Materials & Interfaces* **13**, 49879 (2021).
17. M. Riegraf, F. Han, N. Sata, and R. Costa, *ACS Applied Materials & Interfaces,* **13**, 37239 (2021).
18. R. L. Firor and B. D. Quimby, *Agilent Technologies Inc., USA,* (2001).
19. M. Riegraf, K. Develos-Bagarinao, I. Biswas, and R. Costa, *J. Power Sources,* **559** 232669 (2023).
20. Z. Cheng and M. Liu, *Solid State Ionics*, **178**, 925 (2007).
21. K. Sasaki, K. Susuki, A. Iyoshi, M. Uchimura, N. Imamura, H. Kusaba, Y. Teraoka, H. Fuchino, K. Tsujimoto, Y. Uchida, and N. Jingo, *J. Electrochem. Soc.,* **153**, A2023 (2006).
22. J. H. Wang and M. Liu, *Electrochem. Commun.,* **9**, 2212 (2007).